

Understanding and Improving Virtual Adversarial Training

Dongha Kim *

`dongha0718@hanmail.net`

Yongchan Choi *

`pminer32@gmail.com`

Yongdai Kim *

`ydkim0903@gmail.com`

September 17, 2019

Abstract

In semi-supervised learning, virtual adversarial training (*VAT*) approach is one of the most attractive method due to its intuitional simplicity and powerful performances. *VAT* finds a classifier which is robust to data perturbation toward the adversarial direction. In this study, we provide a fundamental explanation why *VAT* works well in semi-supervised learning case and propose new techniques which are simple but powerful to improve the *VAT* method. Especially we employ the idea of *Bad GAN* approach, which utilizes bad samples distributed on complement of the support of the input data, without any additional deep generative architectures. We generate bad samples of high-quality by use of the adversarial training used in *VAT* and also give theoretical explanations why the adversarial training is good at both generating bad samples. An advantage of our proposed method is to achieve the competitive performances compared with other recent studies with much fewer computations. We demonstrate advantages our method by various experiments with well known benchmark image datasets.

1 Introduction

Deep learning has accomplished unprecedented success due to the development of deep architectures, learning techniques and hardwares Krizhevsky et al. (2012); Ioffe and Szegedy (2015); Szegedy et al. (2015); Hinton et al. (2012); Kingma and Ba (2014). However, deep learning has also suffered from collecting large amount of labeled data which requires both cost and time. Thus it becomes

*Department of Statistics, Seoul National University

important to develop semi-supervised methodologies that learn a classifier (or discriminator) by using small labeled data and large unlabeled data.

Various semi-supervised learning methods have been proposed for deep learning. Weston et al. (2012) employs a manifold embedding technique using the pre-constructed graph of unlabeled data and Rasmus et al. (2015) uses a specially designed auto-encoder to extract essential features for classification. Variational auto encoder Kingma and Welling (2013) is also used in the context of semi-supervised learning by maximizing the variational lower bound of both labeled and unlabeled data Kingma et al. (2014); Maaløe et al. (2016).

Recently, a simple and powerful idea for semi-supervised learning has been proposed, which is called virtual adversarial training (*VAT*, Miyato et al. (2015, 2017)). *VAT* succeeds the core idea of the adversarial training method (Goodfellow et al., 2014b) for supervised learning case, which enhances the invariance of the classifier with respect to perturbation of inputs, and apply this idea to semi-supervised learning case. There are several follow-up studies utilizing *VAT* to sequential data or combining *VAT* with their own method in order to strengthen predicting performances (Miyato et al., 2016; Clark et al., 2018). Though *VAT* is intuitively simple and has powerful performances, it is not still clear why *VAT* works well in semi-supervised learning case.

Semi-supervised learning based on generative adversarial networks (*GAN*, Goodfellow et al. (2014a)) has also received much attention. For K -class classification problems, Salimans et al. (2016) solves the $(K + 1)$ -class classification problem where the additional $(K + 1)$ th class consists of synthetic images made by a generator of the *GAN* learned by unlabeled data. Dai et al. (2017) notices that not a good generator but a bad generator which generates synthetic images much different from observed images is crucial, and develops a semi-supervised learning algorithm called *Bad GAN* which achieves great performances over multiple benchmark datasets. However, *Bad GAN* needs two additional deep architectures - bad generator and pre-trained density estimation model besides the one for the classifier. Learning these multiple deep architectures requires huge computation and memory consumption. In particular, the *PixelCNN++* Salimans et al. (2017) is used for the pre-trained density estimation model which consumes very large computational resources.

In this study, we give fundamental explanations why *VAT* works well for semi-supervised learning case. One of the standard assumption for semi-supervised learning is *cluster assumption* which means the optimal decision boundary locates at low density regions Chapelle et al. (2006). We find that *VAT* pushes the decision boundary away from the high density regions of data and thus helps to find a desirable classifier given the *cluster assumption*. To be more specific, the objective function of the *VAT* method can be interpreted as a differentiable version of the ideal loss function whose optimizer is a perfect classifier.

Based on the findings, we propose new techniques to enhance the performance of *VAT*. First we employ the idea of *Bad GAN*, which utilizes bad samples distributed on complement of the support of input data, without any additional deep generative architectures. Our proposed technique is

motivated by close investigation of adversarial direction in *VAT*. Here, the adversarial direction for a given datum is the direction to which the probabilities of each class change most. We prove that the perturbed data toward their adversarial directions can serve as ‘good’ bad samples. Dai et al. (2017) proves that bad samples play a role to pull the decision boundary toward the low density regions of data. By using the adversarial directions for both measuring invariance and generating the bad samples, the proposed method combines the advantages of *VAT* and *Bad GAN* together. That is, our method accelerates the learning procedure by using both pushing and pulling operations simultaneously.

Secondly we modify the approximation method to calculate the adversarial direction in Miyato et al. (2017). Miyato et al. (2017) propose the approximation method by using the second-order Taylor expansion. We modify the idea by considering the reverse directions of dominant eigenvectors and find that the slight modification helps to improve the *VAT* method. We call the modified *VAT* with newly proposed techniques *FAT* (Fast Adversarial Training). We show that *FAT* achieves almost the state-of-the-art performances with much fewer training epochs. Especially, for the MNIST dataset, *FAT* achieves similar test accuracies to those of *Bad GAN* and *VAT* with 5 times and 7 times fewer training epochs, respectively.

This paper is organized as follows. In Section 2, we review the *VAT* and *Bad GAN* methods briefly. Theoretical analysis of *VAT* is given in Section 3. In Section 4, the technique to generate bad samples using the adversarial directions is described, and our proposed semi-supervised learning method is presented. Results of various experiments are presented in Section 5 and conclusions follow in Section 6.

2 Related works

2.1 *VAT* approach

VAT Miyato et al. (2017) is a regularization method which is inspired by the adversarial training (Goodfellow et al., 2014b). The regularization term of *VAT* is given as:

$$\begin{aligned} L^{\text{VAT}}(\theta; \hat{\theta}, \mathbf{x}, \epsilon) &= D_{\text{KL}}\left(p(\cdot|\mathbf{x}; \hat{\theta})\|p(\cdot|\mathbf{x} + \mathbf{r}_{\text{advr}}(\mathbf{x}, \epsilon); \theta)\right) \\ &= -\sum_{k=1}^K p(k|\mathbf{x}; \hat{\theta}) \log p(k|\mathbf{x} + \mathbf{r}_{\text{advr}}(\mathbf{x}, \epsilon); \theta) + C, \end{aligned}$$

where

$$\mathbf{r}_{\text{advr}}(\mathbf{x}, \epsilon) = \underset{\mathbf{r}; \|\mathbf{r}\| \leq \epsilon}{\text{argmax}} D_{\text{KL}}\left(p(\cdot|\mathbf{x}; \hat{\theta})\|p(\cdot|\mathbf{x} + \mathbf{r}; \theta)\right), \quad (1)$$

$\epsilon > 0$ is a tuning parameter, θ is the parameter in the discriminator to train, $\hat{\theta}$ is the current estimate of θ and C is a constant. Combining with the cross-entropy term of the labeled data, we get the

final objective function of *VAT*:

$$-\mathbb{E}_{\mathbf{x}, y \sim \mathcal{L}^{tr}} [\log p(y|\mathbf{x}; \theta)] + \mathbb{E}_{\mathbf{x} \sim \mathcal{U}^{tr}} \left[L^{\text{VAT}}(\theta; \hat{\theta}, \mathbf{x}, \epsilon) \right], \quad (2)$$

where \mathcal{L}^{tr} and \mathcal{U}^{tr} are labeled and unlabeled datasets respectively.

2.2 *Bad GAN* approach

Bad GAN Dai et al. (2017) is a method that trains a good discriminator with a bad generator. Let $\mathcal{D}_G(\phi)$ be generated bad samples with a bad generator $p_G(\cdot; \phi)$ parametrized by ϕ . Here, the ‘bad generator’ is a deep architecture to generate samples different from observed data. Let $p^{\text{pt}}(\cdot)$ be a pre-trained density estimation model. For a given discriminator with a feature vector $v(\mathbf{x}; \theta)$ of a given input x parameterized by θ , *Bad GAN* learns the bad generator by minimizing the following:

$$\mathbb{E}_{\mathbf{x} \sim \mathcal{D}_G(\phi)} [\log p^{\text{pt}}(\mathbf{x}) \mathbb{I}(p^{\text{pt}}(\mathbf{x}) > \tau)] + \|\mathbb{E}_{\mathbf{x} \sim \mathcal{U}^{tr}} v(\mathbf{x}; \hat{\theta}) - \mathbb{E}_{\mathbf{x} \sim \mathcal{D}_G(\phi)} v(\mathbf{x}; \hat{\theta})\|^2$$

with respect to ϕ , where $\tau > 0$ is a tuning parameter, \mathcal{U}^{tr} is the unlabeled data, and $\hat{\theta}$ is the current estimate of θ and $\|\cdot\|$ is the Euclidean norm.

In turn, to train the discriminator, we consider the K -class classification problem as the $(K + 1)$ -class classification problem where the $(K + 1)$ -th class is an artificial label of the bad samples generated by the bad generator. We estimate the parameter θ in the discriminator by minimizing the following:

$$\begin{aligned} & -\mathbb{E}_{\mathbf{x}, y \sim \mathcal{L}^{tr}} [\log p(y|\mathbf{x}, y \leq K; \theta)] - \mathbb{E}_{\mathbf{x} \sim \mathcal{U}^{tr}} \left[\log \left\{ \sum_{k=1}^K p(k|\mathbf{x}; \theta) \right\} \right] \\ & -\mathbb{E}_{\mathbf{x} \sim \mathcal{D}_G(\phi)} [\log p(K + 1|\mathbf{x}; \theta)] - \mathbb{E}_{\mathbf{x} \sim \mathcal{U}^{tr}} \left[\sum_{k=1}^K p(k|\mathbf{x}; \theta) \log p(k|\mathbf{x}; \theta) \right] \end{aligned} \quad (3)$$

for given ϕ , where \mathcal{L}^{tr} is the labeled set. See Dai et al. (2017) for details of the objective function (3).

3 Investigation of *VAT* for semi-supervised learning

In this section, we give a theoretical insight for the role of the regularization term of *VAT* in semi-supervised learning. We show that the regularization term of *VAT* pushes the decision boundary from the high density regions of unlabeled data and thus helps to find a desirable classifier given the *cluster assumption*.

3.1 Theoretical analysis of *VAT*

Let (\mathcal{X}, d) be a given metric space and $(X, Y) \in \mathcal{X} \times \{1, \dots, K\}$ be input and output random variables with a density function $p(\mathbf{x}, y)$. We assume that $p(\mathbf{x}|y = k)$ is positive and continuous

on \mathcal{X} and $p(y = k) > 0$ for all k . For $a > 0$ define $\mathcal{X}(a) := \cup_{k=1}^K \mathcal{X}_k(a)$ and $\delta(a) := \Pr(X \in \mathcal{X} - \mathcal{X}(a))$ where $\mathcal{X}_k(a) := \left\{ \mathbf{x} \in \mathcal{X} : \Pr(Y = k|\mathbf{x}) - \max_{k' \neq k} \Pr(Y = k'|\mathbf{x}) > a \right\}$. And also define P_a the probability measure of truncated random variable X on $\mathcal{X}(a)$ whose density function is given as $p_a(\mathbf{x}) \propto p(\mathbf{x}) \cdot \mathbb{I}(\mathbf{x} \in \mathcal{X}(a))$.

For a given function $f : \mathcal{X} \rightarrow \mathbb{R}^K$, let $C(\cdot; f) : \mathcal{X} \rightarrow \{1, \dots, K\}$ be an induced classifier defined as $C(\mathbf{x}; f) := \operatorname{argmax}_{k=1, \dots, K} f_k(\mathbf{x})$ and let $C^B(\cdot)$ be the Bayes classifier. We denote the decision boundary of a given induced classifier $C(\cdot; f)$ by $D(f)$ and the decision boundary of the Bayes classifier by D^B .

Let $(X_1, Y_1), \dots, (X_n, Y_n)$ be n independent copies from (X, Y) . We propose two measures of a given function f : one is a standard empirical risk of labeled data given as $l_n(f) := \frac{1}{n} \sum_{i=1}^n \mathbb{I}(C(X_i; f) \neq Y_i)$, and the other is an invariance measure of perturbation defined as

$$u_{a, \epsilon}(f) := \mathbb{E}_{P_a} [\mathbb{I}(C(\mathbf{x}; f) \neq C(\mathbf{x} + \mathbf{r}; f) \text{ for all } \mathbf{r} \in \mathcal{B}(0, \epsilon))], \quad (4)$$

where $a, \epsilon > 0$ and $\mathcal{B}(0, \epsilon) := \{\mathbf{v} : d(0, \mathbf{v}) < \epsilon\}$.

Now we are ready to establish a proposition which means that the classifier which is invariant with respect to all small perturbations and classifies the labeled data correctly converges to the Bayes classifier exponentially fast with the number of labeled data. The proof is in the supplementary materials.

Proposition 1 *Let \mathcal{F} be a set of continuous functions including f^B whose corresponding classifier is the Bayes classifier. For $a, \epsilon > 0$, let $\hat{f}_n \in \operatorname{argmin}_{f \in \mathcal{F}_{a, \epsilon}} l_n(f)$, where $\mathcal{F}_{a, \epsilon} := \left\{ f \in \mathcal{F} : f \in \operatorname{argmin}_{f \in \mathcal{F}} u_{a, \epsilon}(f) \right\}$. Then there exist $\delta^*, \epsilon^*, c_1^*, c_2^* > 0$ not depending on n , if $\delta(a) < \delta^*$ and $\epsilon < \epsilon^*$, then*

$$P^{(n)} \left[\Pr \left(C(X; \hat{f}_n) = C^B(X) \right) \geq 1 - \delta(a) \right] \geq 1 - c_2^* \exp(-nc_1^*/2), \quad (5)$$

where $P^{(n)}$ is the product probability measure of $(X_1, Y_1), \dots, (X_n, Y_n)$.

Note that the Bayes decision boundary D^B locates at $\mathcal{X} - \mathcal{X}(a)$, hence the small value of $\delta(a)$ means essentially the *cluster assumption*. The term $u_{a, \epsilon}(f)$ encourages the decision boundary not to be located inside the support $\mathcal{X}(a)$ or equivalently pushes the decision boundary from the high density regions of data, which results to find a good classifier given the *cluster assumption*.

3.2 Interpretation of VAT

Here we claim that the objective terms in VAT can be interpreted as modified version of l_n and $u_{\eta, \epsilon}$ respectively. Let $f(\mathbf{x}; \theta) := (p(y = k|\mathbf{x}; \theta))_{k=1}^K$ and $C(\mathbf{x}; \theta) := \operatorname{argmax}_k f_k(\mathbf{x}; \theta)$. Proposition 1 implies that it would be good to pursue a classifier which predicts the labeled data correctly and at the same time is invariant with respect to all local perturbations on the unlabeled data. For this purpose, a plausible candidate of the objective function is

$$\mathbb{E}_{(\mathbf{x}, y) \sim \mathcal{L}^{tr}} [\mathbb{I}(y \neq C(\mathbf{x}; \theta))] + \mathbb{E}_{\mathbf{x} \sim \mathcal{U}^{tr}} [\mathbb{I}(C(\mathbf{x}; \theta) \neq C(\mathbf{x} + \mathbf{r}; \theta) \text{ for all } \mathbf{r} \in \mathcal{B}(0, \epsilon))], \quad (6)$$

where \mathcal{L}^{tr} and \mathcal{U}^{tr} are labeled data and unlabeled data respectively.

The objective function (6) is not practically usable since neither optimizing the indicator function nor checking $C(\mathbf{x}; \theta) \neq C(\mathbf{x} + \mathbf{r}; \theta)$ for all \mathbf{r} in $\mathcal{B}(0, \epsilon)$ is possible. To resolve these problems, we replace the indicator functions in (6) with the cross-entropies, and the neighborhood $\mathcal{B}(\mathbf{x}, \epsilon)$ in the second term with the adversarial direction. By doing so, we have the following alternative objective function:

$$-\mathbb{E}_{(\mathbf{x}, y) \sim \mathcal{L}^{tr}} [\log p(y|\mathbf{x}; \theta)] - \mathbb{E}_{\mathbf{x} \sim \mathcal{U}^{tr}} \left[\sum_{k=1}^K p(k|\mathbf{x}; \theta) \log p(k|\mathbf{x} + \mathbf{r}_{\text{advr}}(\mathbf{x}, \epsilon); \theta) \right]. \quad (7)$$

Finally, we replace $p(\cdot|\mathbf{x}; \theta)$ in the second term of (7) by $p(\cdot|\mathbf{x}; \hat{\theta})$ to have the objective function of VAT (2).

4 Improved techniques for VAT

4.1 Generation of bad samples by adversarial training

The key role of bad samples in *Bad GAN* is to enforce the decision boundary to be pulled toward the low density regions of the unlabeled data. In this section, we propose a novel technique to generate ‘good’ bad samples by use of only a given classifier.

4.1.1 Motivation

Let us consider the 2-class linear logistic regression model parametrized by $\eta = \{\mathbf{w}, b\}$, that is, $p(y = 1|x; \eta) = \left(1 + \exp(-b - \mathbf{w}'\mathbf{x})\right)^{-1}$. Note that the decision boundary is $\{\mathbf{x} : b + \mathbf{w}'\mathbf{x} = 0\}$, and for any given \mathbf{x} , the distance between \mathbf{x} and the decision boundary is $|b + \mathbf{w}'\mathbf{x}|/\|\mathbf{w}\|$. The key result is that moving \mathbf{x} toward the adversarial direction $\mathbf{r}_{\text{advr}}(\mathbf{x}, \epsilon)$ is equivalent to moving \mathbf{x} toward the decision boundary which is stated rigorously in the following proposition. The proof is in the supplementary materials.

Proposition 2 *For a sufficiently small $\epsilon > 0$, we have*

$$|b + \mathbf{w}'\mathbf{x}|/\|\mathbf{w}\| > |b + \mathbf{w}'(\mathbf{x} + \mathbf{r}^{\text{advr}}(\mathbf{x}, \epsilon))|/\|\mathbf{w}\|$$

unless $|b + \mathbf{w}'\mathbf{x}| = 0$.

Hence, we can treat $\mathbf{x} + C\mathbf{r}_{\text{advr}}(\mathbf{x}, \epsilon)/\|\mathbf{r}^{\text{advr}}(\mathbf{x}, \epsilon)\|$ for appropriately choosing $C > 0$ as a bad sample. For the decision boundary made by the DNN model with ReLU activation function, see the supplementary materials.

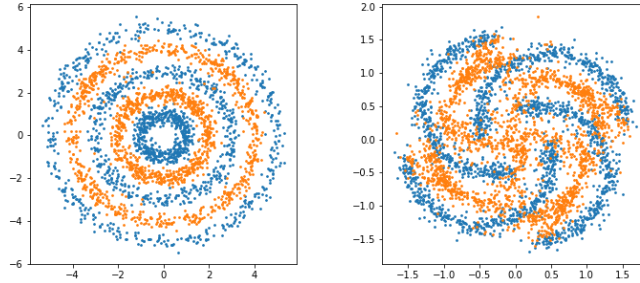


Figure 1: Demonstration of how the bad samples generated by the adversarial training are distributed. We consider two cases: 3-class classification problem (**Left**) and 4-class classification problem (**Right**). True data and bad data are coloured by blue and orange, respectively.

4.1.2 Bad sample Generation with general classifier

Motivated by Proposition 2, we propose a bad sample generator as follows. Let $C > 0$ be fixed and $\hat{\theta}$ be the current estimate of θ . For a given datum \mathbf{x} and a classifier $p(\cdot|\mathbf{x};\hat{\theta})$, we calculate the adversarial direction $\mathbf{r}_{\text{advr}}(\mathbf{x}, \epsilon)$ for given ϵ by (1). Then, we consider $\mathbf{x}_{\text{bad}} = \mathbf{x} + C\mathbf{r}_{\text{advr}}(\mathbf{x}, \epsilon)/\|\mathbf{r}_{\text{advr}}(\mathbf{x}, \epsilon)\|$ as a bad sample. It may happen that a generated bad sample is not sufficiently close to the decision boundary to be a 'good' bad sample, in particular when C is too large or too small. To avoid such a situation, we exclude \mathbf{x}_{art} which satisfies the following condition for a pre-specified $\alpha > 0$:

$$\max_k p(k|\mathbf{x}_{\text{bad}};\hat{\theta}) > 1 - \alpha.$$

In Figure 1, we illustrate how the bad samples generated by the proposed adversarial training are distributed for multi-class problem. With a good classifier, we can clearly see that most bad samples are located well in the low density regions of the data.

Remark 1 *Note that samples near the decision boundary are not always located in low density regions. Samples near the decision boundary are served as bad samples only with the reasonable classifier. In order to reflect this finding to learning procedure, we employ the warm-up technique which is described in Section 4.*

4.2 Modified approximation method of the adversarial direction

Miyato et al. (2017) proposes the fast approximation method to calculate the adversarial direction $\mathbf{r}_{\text{advr}}(\mathbf{x}, \epsilon)$ by using the second-order Taylor expansion. Let us define $H(\mathbf{x}, \hat{\theta}) = \nabla\nabla D_{\text{KL}}\left(p(\cdot|\mathbf{x};\hat{\theta})\|p(\cdot|\mathbf{x} + \mathbf{r};\hat{\theta})\right)|_{\mathbf{r}=\mathbf{0}}$. They claim that \mathbf{r}_{advr} emerges as the first dominant eigenvector $v(\mathbf{x}, \hat{\theta})$ of $H(\mathbf{x}, \hat{\theta})$ with magnitude ϵ . But there always exist two dominant eigenvectors, $\pm v(\mathbf{x}, \hat{\theta})$, and the sign should be selected carefully.

So, we slightly modify the approximation method of Miyato et al. (2017) by

$$\mathbf{r}_{\text{advr}}(\mathbf{x}, \epsilon) = \underset{\mathbf{r} \in \{v(\mathbf{x}, \hat{\theta}), -v(\mathbf{x}, \hat{\theta})\}}{\text{argmax}} D_{\text{KL}} \left(p(\cdot | \mathbf{x}; \hat{\theta}) || p(\cdot | \mathbf{x} + \mathbf{r}; \hat{\theta}) \right).$$

4.3 Proposed objective function

With the new techniques described in Section 4, our proposed method called *FAT* updates θ by minimizing the following objective function:

$$\begin{aligned} & -\mathbb{E}_{\mathbf{x}, y \sim \mathcal{L}^{\text{tr}}} [\log p(y | \mathbf{x}; \theta)] + \mathbb{E}_{\mathbf{x} \sim \mathcal{U}^{\text{tr}}} [L^{\text{VAT}}(\theta; \hat{\theta}, \mathbf{x}, \epsilon)] \\ & + \lambda \cdot [\mathbb{E}_{\mathbf{x} \sim \mathcal{U}^{\text{tr}}} [L^{\text{true}}(\theta; \mathbf{x})] + \mathbb{E}_{\mathbf{x} \sim \mathcal{D}^{\text{bad}}(\hat{\theta}, \epsilon, C)} [L^{\text{fake}}(\theta, \mathbf{x})]] \end{aligned} \quad (8)$$

where $\mathcal{D}^{\text{bad}}(\hat{\theta}, \epsilon, C)$ is the set of generated bad samples with $\hat{\theta}, \epsilon$ and C ,

$$\begin{aligned} L^{\text{true}}(\theta; \mathbf{x}) &= -\sum_{k=1}^K \left[\frac{\exp(g_k(\mathbf{x}; \theta))}{1 + \sum_{k'=1}^K \exp(g_{k'}(\mathbf{x}; \theta))} \log \frac{\exp(g_k(\mathbf{x}; \theta))}{1 + \sum_{k'=1}^K \exp(g_{k'}(\mathbf{x}; \theta))} \right], \\ L^{\text{fake}}(\theta; \mathbf{x}) &= -\log \frac{1}{1 + \sum_{k=1}^K \exp(g_k(\mathbf{x}; \theta))}, \end{aligned}$$

$g(\mathbf{x}; \theta) \in \mathbb{R}^K$ is a pre-softmax vector of a given architecture and $\lambda > 0$. We treat ϵ and C as tuning parameters to be selected based on the validation data accuracy. Note that L^{fake} has the same role as the sum of third and fourth terms in (3).

As described in Remark 1, \mathbf{x}_{bad} s are distributed in low density regions only when the classifier performs well, which means \mathbf{x}_{bad} s hamper the learning procedure at early learning phase. Thus we use the *warm-up* strategy Bowman et al. (2015), that is, we start with the small λ being 0 and increase it gradually after learning step proceeds.

5 Experiments

5.1 Prediction performance comparisons

We compare prediction performances of *FAT* over the benchmark datasets with other semi-supervised learning algorithms. We consider the most widely used datasets: MNIST (LeCun et al., 1998), SVHN (Marlin et al., 2010) and CIFAR10 (Krizhevsky and Hinton, 2009). For fair comparison, we use the same architectures as those used in Miyato et al. (2017) for MNIST, SVHN and CIFAR10. See the supplementary materials for details. The optimal tuning parameters (ϵ, C, α) in *FAT* are chosen based on the validation data accuracy. We set λ by zero and increase it by 0.1 after every training epoch up to one. We use *Adam* algorithm (Kingma and Ba, 2014) to update the parameters and do not use any data augmentation techniques. The results are summarized in Table 1, which shows that *FAT* achieves the state-of-the-art accuracies for MNIST (20) and SVHN (500, 1000)

Table 1: Prediction accuracies of various semi-supervised learning algorithms for the three benchmark datasets. $|\mathcal{L}|$ is the number of labeled data and the results with * are implemented by us.

Data $ \mathcal{L} $	Test acc.(%)					
	MNIST		SVHN		CIFAR10	
	20	100	500	1000	1000	4000
<i>DGN</i> (Kingma et al., 2014)	-	96.67	-	63.98	-	-
<i>Ladder</i> (Rasmus et al., 2015)	-	98.94	-	-	-	79.6
<i>FM-GAN</i> (Salimans et al., 2016)	83.23	99.07	81.56	91.89	78.13	81.37
<i>FM-GAN-Tan</i> (Kumar et al., 2017)	-	-	95.13	95.61	80.48	83.80
<i>Bad GAN</i> (Dai et al., 2017)	80.16*	99.20	-	95.75	-	85.59
<i>VAT</i> (Miyato et al., 2017)	67.04*	98.64	-	93.17	-	85.13
<i>Tri-GAN</i> (LI et al., 2017)	95.19	99.09	-	94.23	-	83.01
<i>CCLP</i> (Kamnitsas et al., 2018)	-	99.25	-	94.31	-	81.43
<i>FAT</i>	96.32	98.89	95.21	95.94	78.44	85.31

and competitive accuracies with the state-of-the-art method for other settings. Since *FAT* only needs one deep architecture, we can conclude that *FAT* is a powerful and computationally efficient method.

An other advantage of *FAT* is its stability with respect to learning phase. With small labeled data, Figure 2 shows that the test accuracies of each epoch tends to fluctuate much and be degraded for *VAT* and *Bad GAN* while *FAT* provides much more stable result. This may be partly because the bad samples helps to stabilize the objective function.

5.2 Effects of tuning parameters

FAT introduces three tuning parameters ϵ, C and α , where ϵ is the constant used to find the adversarial direction, C is the radius to generate artificial samples and α is used to determine whether an artificial sample is 'good'. We investigate the sensitivities of prediction performances with respect to the changes of the values of these tuning parameters. When we vary one of the tuning parameters, the other parameters are fixed at the optimal values chosen by the validation data. The results are reported in Table 2. Unless α is too small or too large, the prediction performances are not changed much. For ϵ and C , care should be done. With c larger than the optimal C (i.e. 2) or with C smaller than the optimal ϵ (i.e. 1.5), the prediction performances are suboptimal. Apparently, choosing ϵ and C with ϵ being slightly smaller than C gives the best result.

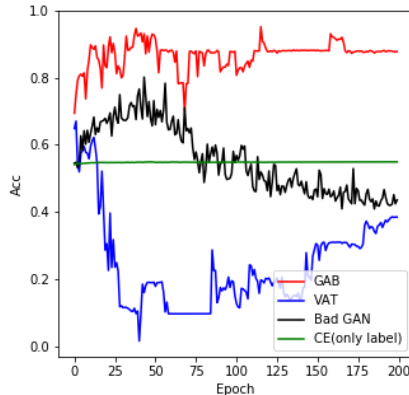


Figure 2: Trace plot of the test accuracies for MNIST with 20 labeled data.

Table 2: Test accuracies of MNIST (100) for various values of ϵ , C and α . The other parameters on each case are fixed to the optimal values.

c	1.	1.5	2.	4.
Test acc.	97.94	98.89	98.61	95.65
C	1	2.	4.	6.
Test acc.	89.54	98.89	98.79	98.55
α	0.001	0.01	0.1	0.2
Test acc.	98.65	98.89	98.77	98.71

Table 3: Learning time per training epoch ratios compared to supervised learning with cross-entropy for CIFAR10. *Bad GAN* is operated without *PixelCNN++*.

Method	<i>VAT</i>	<i>FAT</i>	<i>Bad GAN</i>
Time ratio	1.37	2.09	3.20

5.3 Computational efficiency

We investigate the computational efficiency of our method in view of learning speed and computation time per training epoch. For *Bad GAN*, we did not use *PixelCNN++* on SVHN and CIFAR10 datasets since the pre-trained *PixelCNN++* models are not publicly available. Without *PixelCNN++*, *Bad GAN* is similar to *FM-GAN* (Salimans et al., 2016). Figure 3 draws the bar plots about the numbers of epochs needed to achieve the pre-specified test accuracies. We can clearly see that *FAT* requires much less epochs.

We also calculate the ratios of the computing time of each semi-supervised learning algorithm over the computing time of the corresponding supervised learning algorithm for CIFAR10 dataset, whose results are summarized in Table 3. These ratios are almost same for different datasets. The computation time of *FAT* is less than *Bad GAN* and competitive to *VAT*. From the results of Figure 3 and Table 3 we can conclude that *FAT* achieves the pre-specified performances efficiently. Note

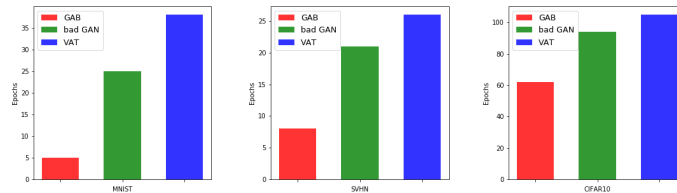


Figure 3: The number of epochs to achieve the pre-specified test accuracies (98%, 90% and 80%) with the three methods for **(Left)** MNIST (100), **(Middle)** SVHN (1000) and **(Right)** CIFAR10 (4000) settings. *Bad GAN* is operated without *PixelCNN++* for SVHN and CIFAR10 datasets.

that the learning time of *PixelCNN++* is not considered for this experiment, and so comparison of computing time of *FAT* and *Bad GAN* with *PixelCNN++* is meaningless.

5.4 Improvement of bad samples with VAT

For generated samples by adversarial training to be ‘good’ bad samples, the adversarial directions should be toward the decision boundary. While this always happens for the linear model by Proposition 2, adversarial directions could be opposite to the decision boundary for deep model. To avoid such undesirable cases as much as possible, it would be helpful to smoothen the classifier with a regularization term. Here, we claim that the regularization term of *VAT* plays such a role.

The adversarial direction obtained by maximizing the KL divergence is sensitive to local fluctuations of the class probabilities which is exemplified in Figure 4. The regularization term of *VAT* is helpful to find a right adversarial direction which is toward the decision boundary by eliminating unnecessary local fluctuations of the class probabilities. In Figure 5, we compare bad samples generated by the adversarial training with and without the regularization term of *VAT* for the MNIST dataset. While the bad samples generated without the regularization term of *VAT* are visually similar to the given input vectors, the bad samples generated with the regularization term of *VAT* look like mixtures of two different digits and thus serve as ‘better’ bad samples.

5.5 Quality of bad samples

We investigate how ‘good’ artificial samples generated by *FAT* are. The left two plots of Figure 6 shows the scatter plot of the synthetic data and the trace plot of prediction accuracies of *FAT* and *VAT*. And the right four plots of Figure 6 draws the scatter plots with generated artificial samples at various epochs. We can clearly see that artificial samples are distributed near the current decision boundary. We also compare artificial images generated by *FAT* and bad images generated by *Bad GAN* for the MNIST data at the end of learning procedure. In Figure 7, the images by *FAT* do not look like real images and do not seem to be collapsed, which indicates that *FAT* consistently

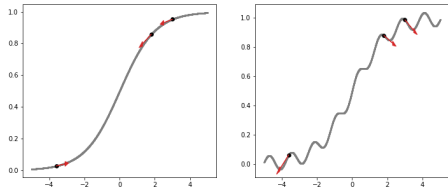


Figure 4: Examples of $P(y = 1|x)$ of smooth (**Left**) and wiggle (**Right**) cases. We plot 3 points and their adversarial directions on each case.

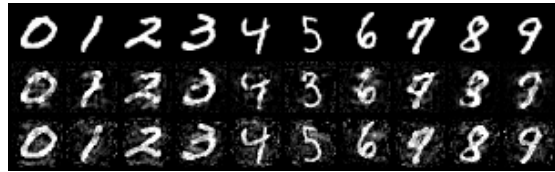


Figure 5: (**Upper**) 10 randomly sampled original MNIST dataset. (**Middle and Lower**) Bad samples obtained by the classifier learned with and without the regularization term of VAT.

generates diverse and good artificial samples. *Bad GAN* also generates diverse bad samples but some ‘realistic’ images can be found.

6 Conclusion

In this paper, we give fundamental explanations why *VAT* works well for semi-supervised learning case. *VAT* pushes the decision boundary from the high density regions of data, which results to find a good classifier given the *cluster assumption*. Also we propose a new method for semi-supervised learning, called *FAT*, which modifies *VAT* by introducing simple but powerful techniques. *FAT* is devised to compromise the advantages of *VAT* and *Bad GAN* together. In numerical experiments, we show that *FAT* achieves almost the state-of-the-art performances with much fewer epochs.

Unlike *Bad GAN*, *FAT* only needs to learn a discriminator. Hence, it could be extended without much effort to other learning problems. For example, *FAT* can be modified easily for recurrent neural networks and hence can be applied to sequential data. We will leave this extension as a future work.

Acknowledgments

This work is supported by Samsung Electronics Co., Ltd.

References

- Bowman, S. R., Vilnis, L., Vinyals, O., Dai, A. M., Jozefowicz, R., and Bengio, S. (2015). Generating sentences from a continuous space. *arXiv preprint arXiv:1511.06349*.
- Chapelle, O., Schölkopf, B., and Zien, A., editors (2006). *Semi-Supervised Learning*. MIT Press, Cambridge, MA.

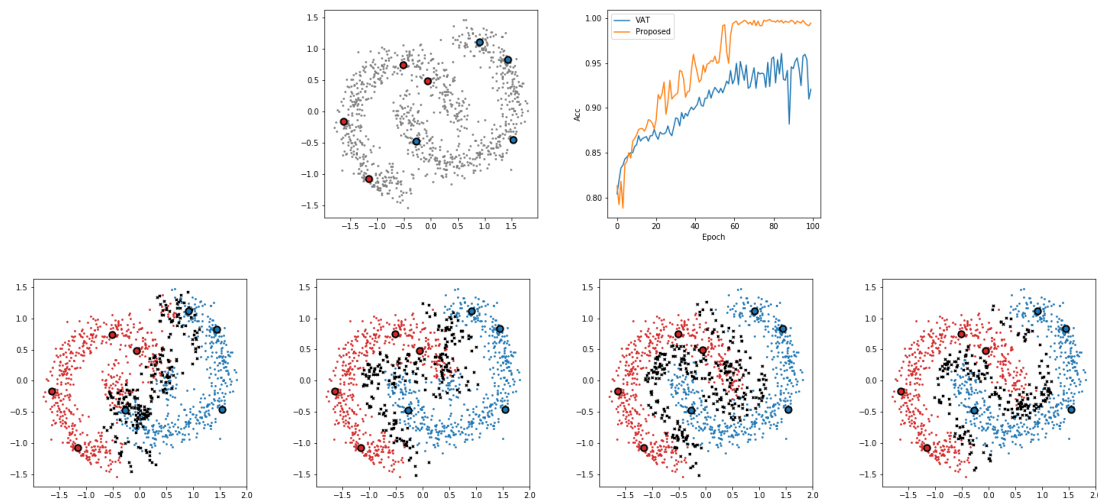


Figure 6: **(Upper left)** The scatter plot of synthetic data which consist of 1000 unlabeled data (gray) and 4 labeled data for each class (red and blue with black edge). **(Upper right)** Accuracies of unlabeled data for each epochs for *VAT* and *FAT*. We use 2-layered NN with 100 hidden units each. **(Lower)** Artificial samples and classified unlabeled data by colors at the 20,40,60 and 80 training epochs of *FAT* respectively.

Clark, K., Luong, T., and Le, Q. V. (2018). Cross-view training for semi-supervised learning.

Dai, Z., Yang, Z., Yang, F., Cohen, W. W., and Salakhutdinov, R. R. (2017). Good semi-supervised learning that requires a bad gan. In *Advances in Neural Information Processing Systems*, pages 6513–6523.

Goodfellow, I., Pouget-Abadie, J., Mirza, M., Xu, B., Warde-Farley, D., Ozair, S., Courville, A., and Bengio, Y. (2014a). Generative adversarial nets. In *Advances in neural information processing systems*, pages 2672–2680.

Goodfellow, I. J., Shlens, J., and Szegedy, C. (2014b). Explaining and harnessing adversarial examples. *arXiv preprint arXiv:1412.6572*.

He, K., Zhang, X., Ren, S., and Sun, J. (2015). Delving deep into rectifiers: Surpassing human-level performance on imagenet classification. In *Proceedings of the IEEE international conference on computer vision*, pages 1026–1034.

Hinton, G. E., Srivastava, N., Krizhevsky, A., Sutskever, I., and Salakhutdinov, R. R. (2012).



Figure 7: 100 randomly sampled artificial images and bad images with **(Left)** *FAT* and **(Right)** *Bad GAN* respectively.

Improving neural networks by preventing co-adaptation of feature detectors. *arXiv preprint arXiv:1207.0580*.

Ioffe, S. and Szegedy, C. (2015). Batch normalization: Accelerating deep network training by reducing internal covariate shift. *arXiv preprint arXiv:1502.03167*.

Kamnitsas, K., Castro, D., Folgoc, L. L., Walker, I., Tanno, R., Rueckert, D., Glocker, B., Criminisi, A., and Nori, A. (2018). Semi-supervised learning via compact latent space clustering. In Dy, J. and Krause, A., editors, *Proceedings of the 35th International Conference on Machine Learning*, volume 80 of *Proceedings of Machine Learning Research*, pages 2459–2468.

Kingma, D. P. and Ba, J. (2014). Adam: A method for stochastic optimization. *arXiv preprint arXiv:1412.6980*.

Kingma, D. P., Mohamed, S., Rezende, D. J., and Welling, M. (2014). Semi-supervised learning with deep generative models. In *Advances in Neural Information Processing Systems*, pages 3581–3589.

Kingma, D. P. and Welling, M. (2013). Auto-encoding variational bayes. *arXiv preprint arXiv:1312.6114*.

Krizhevsky, A. and Hinton, G. (2009). Learning multiple layers of features from tiny images. Technical report, Citeseer.

Krizhevsky, A., Sutskever, I., and Hinton, G. E. (2012). Imagenet classification with deep convolutional neural networks. In *Advances in neural information processing systems*, pages 1097–1105.

Kumar, A., Sattigeri, P., and Fletcher, T. (2017). Semi-supervised learning with gans: manifold invariance with improved inference. In *Advances in Neural Information Processing Systems*, pages 5534–5544.

- LeCun, Y., Bottou, L., Bengio, Y., and Haffner, P. (1998). Gradient-based learning applied to document recognition. *Proceedings of the IEEE*, 86(11):2278–2324.
- LI, C., Xu, T., Zhu, J., and Zhang, B. (2017). Triple generative adversarial nets. In Guyon, I., Luxburg, U. V., Bengio, S., Wallach, H., Fergus, R., Vishwanathan, S., and Garnett, R., editors, *Advances in Neural Information Processing Systems 30*, pages 4088–4098.
- Maaløe, L., Sønderby, C. K., Sønderby, S. K., and Winther, O. (2016). Auxiliary deep generative models. *arXiv preprint arXiv:1602.05473*.
- Maas, A. L., Hannun, A. Y., and Ng, A. Y. (2013). Rectifier nonlinearities improve neural network acoustic models. In *Proc. icml*, volume 30, page 3.
- Marlin, B., Swersky, K., Chen, B., and Freitas, N. (2010). Inductive principles for restricted boltzmann machine learning. In *Proceedings of the Thirteenth International Conference on Artificial Intelligence and Statistics*, pages 509–516.
- Miyato, T., Dai, A. M., and Goodfellow, I. (2016). Adversarial Training Methods for Semi-Supervised Text Classification. *ArXiv e-prints*.
- Miyato, T., Maeda, S.-i., Koyama, M., and Ishii, S. (2017). Virtual adversarial training: a regularization method for supervised and semi-supervised learning. *arXiv preprint arXiv:1704.03976*.
- Miyato, T., Maeda, S.-i., Koyama, M., Nakae, K., and Ishii, S. (2015). Distributional smoothing with virtual adversarial training. *arXiv preprint arXiv:1507.00677*.
- Nair, V. and Hinton, G. E. (2010). Rectified linear units improve restricted boltzmann machines. In *Proceedings of the 27th international conference on machine learning (ICML-10)*, pages 807–814.
- Rasmus, A., Berglund, M., Honkala, M., Valpola, H., and Raiko, T. (2015). Semi-supervised learning with ladder networks. In *Advances in Neural Information Processing Systems*, pages 3546–3554.
- Salimans, T., Goodfellow, I., Zaremba, W., Cheung, V., Radford, A., and Chen, X. (2016). Improved techniques for training gans. In *Advances in Neural Information Processing Systems*, pages 2234–2242.
- Salimans, T., Karpathy, A., Chen, X., and Kingma, D. P. (2017). Pixelcnn++: Improving the pixelcnn with discretized logistic mixture likelihood and other modifications. *arXiv preprint arXiv:1701.05517*.
- Szegedy, C., Liu, W., Jia, Y., Sermanet, P., Reed, S., Anguelov, D., Erhan, D., Vanhoucke, V., and Rabinovich, A. (2015). Going deeper with convolutions. In *Proceedings of the IEEE Conference on Computer Vision and Pattern Recognition*, pages 1–9.
- Weston, J., Ratle, F., Mobahi, H., and Collobert, R. (2012). Deep learning via semi-supervised embedding. In *Neural Networks: Tricks of the Trade*, pages 639–655. Springer.

7 Appendix

7.1 Proof of Proposition 1.

Let $d(U, V) := \min_{u \in U, v \in V} d(u, v)$ for two sets U and V . For each $\mathcal{X}_k(a)$, there exists a partition of open sets $\{\mathcal{X}_{kj}(a)\}_{j=1}^{m_k}$ such that

$$\min_{j \neq j'} d(\mathcal{X}_{kj}(a), \mathcal{X}_{kj'}(a)) > 0.$$

Set $\delta^* = a \cdot \min_{k,j} \Pr(X \in \mathcal{X}_{kj}(a))$ and $\epsilon^* = d(\mathcal{X}(a), D^B)$. The proof consists of three steps.

[Step 1.] First we show that if $f \in \mathcal{F}_{a,\epsilon}$ then $d(\mathcal{X}(a), D(f)) \geq \epsilon$. It is easy to check that $u_{a,\epsilon}(f^B) = 0$, which means $u_{a,\epsilon}(f) = 0$ for all $f \in \mathcal{F}_{a,\epsilon}$. Let assume that $d(\mathcal{X}(a), D(f)) < \epsilon$ for some $f \in \mathcal{F}_{a,\epsilon}$. Then there there exists an open ball B such that

$$B \in \mathcal{X}(a) \text{ and } d(B, D(f)) < \epsilon.$$

Since $P_a(B) > 0$, $u_{a,\epsilon}(f) \leq 1 - P_a(B) < 1$, which is a contradiction. Therefore $d(\mathcal{X}(a), D(f)) \geq \epsilon$ for all $f \in \mathcal{F}_{a,\epsilon}$.

We highlight that if f satisfies $d(\mathcal{X}(a), D(f)) \geq \epsilon$, then for any j, k , $C(\mathbf{x}; f)$ is constant on each $\mathcal{X}_{kj}(a)$.

[Step 2.] Let \mathcal{W} be the subset of $\mathcal{X}^n \times \mathcal{Y}^n$ such that

$$\sum_{i=1}^n I(X_i \in \mathcal{X}_{kj}(a), Y_i = k) > \max_{k' \neq k} \left\{ \sum_{i=1}^n I(X_i \in \mathcal{X}_{kj}(a), Y_i = k') \right\} + \sum_{i=1}^n I(X_i \in \mathcal{X} - \mathcal{X}(a)) \quad (9)$$

for all (k, j) , where $\mathcal{Y} := \{1, \dots, K\}$. Note that $C^B(\mathbf{x}) = k$ on $\mathcal{X}_{kj}(a)$ for $j = 1, \dots, m_k$ and $k = 1, \dots, K$. Hence on \mathcal{W} ,

$$\begin{aligned} \sum_{i=1}^n I(Y_i = C^B(X_i), X_i \in \mathcal{X}_{kj}(a)) &= \sum_{i=1}^n I(Y_i = k, X_i \in \mathcal{X}_{kj}(a)) \\ &> \sum_{i=1}^n I(Y_i = k', X_i \in \mathcal{X}_{kj}(a)) + \sum_{i=1}^n I(X_i \in \mathcal{X} - \mathcal{X}(a)) \end{aligned}$$

for any $k' \neq k$. If there exists a tuple (k, j) such that $C(\mathbf{x}; \hat{f}) = k' \neq k$ on $\mathbf{x} \in \mathcal{X}_{kj}(a)$, we have the following inequalities on \mathcal{W} ,

$$\sum_{i=1}^n I(Y_i = C^B(X_i)) \geq \sum_{i=1}^n \sum_{k,j} I(X_i \in \mathcal{X}_{k,j}(a), Y_i = k)$$

and

$$\begin{aligned}
\sum_{i=1}^n I(Y_i = C(X_i; \hat{f})) &\leq \sum_{i=1}^n I(Y_i = C(X_i; \hat{f}), X_i \in \mathcal{X}(a)) + \sum_{i=1}^n I(X_i \in \mathcal{X} - \mathcal{X}(a)) \\
&\leq \sum_{i=1}^n \sum_{(\tilde{k}, \tilde{j}) \neq (k, j)} I(X_i \in \mathcal{X}_{\tilde{k}\tilde{j}}(a), Y_i = \tilde{k}) + \sum_{i=1}^n I(X_i \in \mathcal{X}_{kj}(a), Y_i = k') \\
&\quad + \sum_{i=1}^n I(X_i \in \mathcal{X} - \mathcal{X}(a)).
\end{aligned}$$

Therefore, with (9), we have

$$\sum_{i=1}^n (Y_i = C^B(X_i)) > \sum_{i=1}^n I(Y_i = C(X_i; \hat{f}))$$

on \mathcal{W} , which is contradiction to the definition of \hat{f} . Thus $C(\mathbf{x}; \hat{f}) = C^B(\mathbf{x})$ on $\mathbf{x} \in \mathcal{X}(a)$. Since $\Pr\{X \in \mathcal{X}(a)\} = 1 - \delta(a)$

$$\Pr\{C(X; \hat{f}) = C^B(X)\} \geq 1 - \delta(a)$$

on \mathcal{W} .

[Step 3.] Let $m := \sum_{k=1}^K m_k$ and

$$W_{i,(k,j,k')} := I(X_i \in \mathcal{X}_{kj}(a), Y_i = k) - I(X_i \in \mathcal{X}_{kj}(a), Y_i = k') - I(X_i \in \mathcal{X} - \mathcal{X}(a))$$

for $k' \neq k$. Note that

$$\begin{aligned}
\mathbb{E}(W_{1,(k,j,k')}) &= \int_{\mathcal{X}_{kj}(a)} (p(y = k|\mathbf{x}) - p(y = k'|\mathbf{x})) p(\mathbf{x}) d\mathbf{x} - \delta(a) \\
&> a \cdot \Pr(X \in \mathcal{X}_{kj}(a)) - \delta(a) > 0.
\end{aligned}$$

Let $c_1^* = Km$ and $c_2^* = \min_{k,j} \epsilon \cdot P^0(X \in \mathcal{X}_{kj}(\epsilon)) - \delta(\epsilon)$. Then, Hoeffding's inequality implies that

$$P^{(n)} \left\{ \sum_{i=1}^n W_{i,(k,j,k')} < 0 \right\} \leq \exp(-nc_2^*/2).$$

By the union bound, we have

$$P^{(n)}(\mathcal{W}^c) \leq P^{(n)} \left\{ \min_{k,j,k'} \sum_{i=1}^n W_{i,(k,j,k')} < 0 \right\} \leq c_2^* \cdot \exp(-nc_1^*/2),$$

which complete the proof. \square

7.2 Proof of Proposition 2.

Without loss of generality, we assume that $\mathbf{w}'\mathbf{x} + b > 0$, that is, $p(y = 1|\mathbf{x}; \eta) > p(y = 0|\mathbf{x}; \eta)$. We will show that there exists $c > 0$ such that $\mathbf{w}'\mathbf{r}^{\text{advr}}(\mathbf{x}, \epsilon) < 0$. Note that

$$\begin{aligned} \operatorname{argmax}_{\mathbf{r}, \|\mathbf{r}\| \leq \epsilon, \mathbf{w}'\mathbf{r} > 0} KL(\mathbf{x}, \mathbf{r}; \eta) &= \epsilon \frac{\mathbf{w}}{\|\mathbf{w}\|} (=:\mathbf{r}_1^*) \quad \text{and} \\ \operatorname{argmax}_{\mathbf{r}, \|\mathbf{r}\| \leq \epsilon, \mathbf{w}'\mathbf{r} < 0} KL(\mathbf{x}, \mathbf{r}; \eta) &= -\epsilon \frac{\mathbf{w}}{\|\mathbf{w}\|} (=:\mathbf{r}_2^*). \end{aligned}$$

So all we have to do is to show

$$KL(\mathbf{x}, \mathbf{r}_2^*; \eta) > KL(\mathbf{x}, \mathbf{r}_1^*; \eta).$$

By simple calculation we can get the following:

$$KL(\mathbf{x}, \mathbf{r}_2^*; \eta) - KL(\mathbf{x}, \mathbf{r}_1^*; \eta) = - \left[p(y = 1|\mathbf{x}; \theta) \mathbf{w}'(\mathbf{r}_2^* - \mathbf{r}_1^*) - \log \frac{\exp(\mathbf{w}'(\mathbf{x} + \mathbf{r}_2^*) + b) + 1}{\exp(\mathbf{w}'(\mathbf{x} + \mathbf{r}_1^*) + b) + 1} \right].$$

Using the Taylor's expansion up to the third-order, we obtain the following:

$$\begin{aligned} \log \left[\exp(\mathbf{w}'(\mathbf{x} + \mathbf{r}) + b) + 1 \right] &= \log \left[\exp(\mathbf{w}'\mathbf{x} + b) + 1 \right] + p(y = 1|\mathbf{x}; \eta) \mathbf{w}'\mathbf{r} \\ &\quad + \frac{1}{2} p(y = 1|\mathbf{x}; \eta) p(y = 0|\mathbf{x}; \eta) (\mathbf{w}'\mathbf{r})^2 \\ &\quad - \frac{1}{6} p(y = 1|\mathbf{x}; \eta) p(y = 0|\mathbf{x}; \eta) \{p(y = 1|\mathbf{x}; \eta) - p(y = 0|\mathbf{x}; \eta)\} \sum_{i,j,k=1}^p w_i w_j w_k r_i r_j r_k \\ &\quad + o(\|\mathbf{r}\|^3). \end{aligned}$$

So,

$$\begin{aligned} \log \frac{\exp(\mathbf{w}'(\mathbf{x} + \mathbf{r}_2^*) + b) + 1}{\exp(\mathbf{w}'(\mathbf{x} + \mathbf{r}_1^*) + b) + 1} &= p(y = 1|\mathbf{x}; \eta) \mathbf{w}'(\mathbf{r}_2^* - \mathbf{r}_1^*) \\ &\quad + \frac{1}{3} p(y = 1|\mathbf{x}; \eta) p(y = 0|\mathbf{x}; \eta) \{p(y = 1|\mathbf{x}; \eta) - p(y = 0|\mathbf{x}; \eta)\} \epsilon^3 \|\mathbf{w}\|^3 + o(\epsilon^3). \end{aligned}$$

Thus, we have the following equations:

$$\begin{aligned} KL(\mathbf{x}, \mathbf{r}_2^*; \eta) - KL(\mathbf{x}, \mathbf{r}_1^*; \eta) &= \frac{1}{3} p(y = 1|\mathbf{x}; \eta) p(y = 0|\mathbf{x}; \eta) \{p(y = 1|\mathbf{x}; \eta) - p(y = 0|\mathbf{x}; \eta)\} \epsilon^3 \|\mathbf{w}\|^3 + o(\epsilon^3) \\ &= C^* \cdot \epsilon^3 + o(\epsilon^3). \end{aligned}$$

Therefore, there exists $\epsilon^* > 0$ such that $KL(\mathbf{x}, \mathbf{r}_2^*; \eta) > KL(\mathbf{x}, \mathbf{r}_1^*; \eta)$ for $\forall 0 < \epsilon < \epsilon^*$. \square

7.3 Extension of Proposition 2 for the Deep Neural Networks

Consider a binary classification DNN model with ReLU-like activation function $p(y = 1|\mathbf{x}; \theta) = (1 + \exp(-g(\mathbf{x}; \theta)))^{-1}$ parameterized by θ . Here, ReLU-like function is the activation function which is piece-wise linear, such as ReLU (Nair and Hinton, 2010), lReLU (Maas et al., 2013) and PReLU (He et al., 2015). Since $g(\mathbf{x}; \theta)$ is piecewise linear, we can write $g(\mathbf{x}; \theta)$ as

$$g(\mathbf{x}; \theta) = \sum_{j=1}^N \mathbb{I}(\mathbf{x} \in \mathcal{A}_j) \cdot (\mathbf{w}'_j \mathbf{x} + b_j),$$

where \mathcal{A}_j is a linear region and N is the number of linear regions.

For given \mathbf{x} , suppose $g(\mathbf{x}; \theta) > 0$. If $g(\mathbf{x}; \theta)$ is estimated reasonably, we expect that $g(\mathbf{x}; \theta)$ is decreasing if \mathbf{x} moves toward the decision boundary. A formal statement of this expectation would be that $\mathbf{x} - r \nabla_{\mathbf{x}} g(\mathbf{x}; \theta)$ can arrive at the decision boundary for a finite value of $r > 0$, where $\nabla_{\mathbf{x}}$ is the gradient with respect to \mathbf{x} . Of course, for \mathbf{x} with $g(\mathbf{x}; \theta) < 0$, we expect that $\mathbf{x} + r \nabla_{\mathbf{x}} g(\mathbf{x}; \theta)$ can arrive at the decision boundary for a finite value of $r > 0$. We say that \mathbf{x} is *normal* if there is $r > 0$ such that $\mathbf{x} - r \nabla_{\mathbf{x}} g(\mathbf{x}; \theta) \text{sign}\{g(\mathbf{x}; \theta)\}$ locates at the decision boundary. We say that a linear region \mathcal{A}_j is *normal* if all \mathbf{x} in \mathcal{A}_j are *normal*. We expect that most of \mathcal{A}_j are *normal* if $g(\mathbf{x}; \theta)$ is reasonably estimated so that the probability decreases or increases depending on $\text{sign}\{g(\mathbf{x}; \theta)\}$ if \mathbf{x} is getting closer to the decision boundary.

The following proposition proves that the adversarial direction is toward the decision boundary for all \mathbf{x} s in *normal* linear regions.

Lemma 1 *If a linear region \mathcal{A}_j is normal. Then for any $\mathbf{x} \in \text{int}(\mathcal{A}_j)$, there exists $\epsilon > 0$ and $C > 0$ such that $\mathbf{x}^A = \mathbf{x} + C \mathbf{r}_{\text{advr}}(\mathbf{x}, \epsilon) / \|\mathbf{r}_{\text{advr}}(\mathbf{x}, \epsilon)\|$ is on the decision boundary.*

Proof) Take $\tilde{\epsilon} > 0$ such that $\mathbf{x} + \mathbf{r} \in \mathcal{A}_j$ for $\forall \mathbf{r} \in B(\mathbf{x}, \tilde{\epsilon})$. Then by Proposition 1, there exists $0 < \epsilon^* < \tilde{\epsilon}$ such that for $\forall 0 < \epsilon < \epsilon^*$,

$$\begin{aligned} \mathbf{r}_{\text{advr}}(\mathbf{x}, \epsilon) &= \epsilon \cdot \text{sign}(-b_j - \mathbf{w}'_j \mathbf{x}) \cdot \frac{\mathbf{w}_j}{\|\mathbf{w}_j\|} \\ &\propto -\nabla_{\mathbf{x}} g(\mathbf{x}; \theta) \text{sign}\{g(\mathbf{x}; \theta)\}. \end{aligned}$$

\mathbf{x} is *normal*, thus there exists $C > 0$ such that $\mathbf{x}^A = \mathbf{x} + C \mathbf{r}_{\text{advr}}(\mathbf{x}, \epsilon) / \|\mathbf{r}_{\text{advr}}(\mathbf{x}, \epsilon)\|$ belongs to the decision boundary. \square

7.4 Model architectures

All model architectures used in experiments are based on Miyato et al. (2017).

7.4.1 MNIST

For MNIST dataset, we used fully connected NN with four hidden layers, whose numbers of nodes were (1200,600,300,150) with ReLU activation function (Nair and Hinton, 2010). All the

fully-connected layers are followed by BN(Ioffe and Szegedy, 2015).

7.4.2 SVHN, CIFAR10 and CIFAR100

For SVHN, CIFAR10 and CIFAR100 datasets, we used the CNN architectures. More details are in Table 4.

SVHN	CIFAR10	CIFAR100
32×32 RGB images		
3×3 conv. 64 lReLU	3×3 conv. 96 lReLU	3×3 conv. 128 lReLU
3×3 conv. 64 lReLU	3×3 conv. 96 lReLU	3×3 conv. 128 lReLU
3×3 conv. 64 lReLU	3×3 conv. 96 lReLU	3×3 conv. 128 lReLU
2×2 max-pool, stride 2 dropout, $p = 0.5$		
3×3 conv. 128 lReLU	3×3 conv. 192 lReLU	3×3 conv. 256 lReLU
3×3 conv. 128 lReLU	3×3 conv. 192 lReLU	3×3 conv. 256 lReLU
3×3 conv. 128 lReLU	3×3 conv. 192 lReLU	3×3 conv. 256 lReLU
2×2 max-pool, stride 2 dropout, $p = 0.5$		
3×3 conv. 128 lReLU	3×3 conv. 192 lReLU	3×3 conv. 512 lReLU
1×1 conv. 128 lReLU	1×1 conv. 192 lReLU	1×1 conv. 256 lReLU
1×1 conv. 128 lReLU	1×1 conv. 192 lReLU	1×1 conv. 128 lReLU
global average pool, $6 \times 6 \rightarrow 1 \times 1$		
dense 128 \rightarrow 10	dense 192 \rightarrow 10	dense 128 \rightarrow 100
10-way softmax		100-way softmax

Table 4: CNN models used in our experiments over SVHN, CIFAR10 and CIFAR100. We use leaky ReLU activation function (Maas et al., 2013) and all the convolutional layers and fully-connected layers are followed by BN(Ioffe and Szegedy, 2015).